Monthly Notices of the ROYAL ASTRONOMICAL SOCIETY

MNRAS **430,** 1302–1308 (2013) doi:10.1093/mnras/sts706

Intranight optical variability of radio-quiet weak emission line quasars

Gopal-Krishna,[1] Ravi Joshi[2] and Hum Chand[2]★

[1] *National Centre for Radio Astrophysics (TIFR), Pune University Campus, Pune 411007, India*
[2] *Aryabhatta Research Institute of Observational Sciences (ARIES), Manora Peak, Nainital 263129, India*

Accepted 2012 December 21. Received 2012 December 20; in original form 2012 November 2

ABSTRACT

Based on a recently started programme, we report the first search for intranight optical variability (INOV) among radio-quiet 'weak-line-quasars' (RQWLQs). Eight members of this class were observed on 13 nights in the R band, such that each source was monitored continuously at least once for a minimum duration of about 3.5 h, using the recently installed 130-cm telescope at Devasthal, India. Statistical analysis of the differential light curves was carried out using two versions of the F test. Based on the INOV data acquired so far, the RQWLQ population appears to exhibit stronger INOV activity as compared to the general population of radio-quiet quasars, but similar to the INOV known for radio-loud quasars of non-blazar type. To improve upon this early result, as well as extend the comparison to blazars, a factor of ∼2 improvement in the INOV detection threshold would be needed. Such efforts are underway, motivated by the objective to search for the elusive radio-quiet blazars using INOV observations.

Key words: galaxies: active – BL Lacertae objects: general – galaxies: jets – galaxies: photometry – quasars: emission lines – quasars: general.

1 INTRODUCTION

Powerful active galactic nuclei (AGN) whose luminosity across the electromagnetic spectrum is dominated by a Doppler boosted relativistic jet of non-thermal emission are termed as blazars. The two subsets of this class, namely BL Lac objects (BLOs) and highly polarized quasars (HPQs), although differentiated by the equivalent widths of emission lines, share many properties. But, whereas HPQs have an abundant population of weakly polarized quasar counterparts (mostly radio-quiet quasars, called RQQs), various searches for radio-quiet analogs of BLOs have so far remained unsuccessful. BLOs characterized by very weak or absent optical/ultraviolet (UV) emission lines, which have been pursued in such searches, are selected from optical surveys (e.g. Jannuzi, Green & French 1993; Londish et al. 2004), although X-ray-selected BLOs have also been targeted (e.g. Stocke et al. 1990). Usually, the radio loudness is quantified in terms of a parameter R defined as the ratio of the rest-frame 6 cm to 2500 Å flux densities and powerful AGN having $R > 10$ are designated as radio-loud (e.g. Kellermann et al. 1989; Stocke et al. 1992; Jiang et al. 2007; Shen et al. 2011). The first radio-quiet AGN showing weak emission lines, to be interpreted as a non-BLO was PG 1407+265 at $z = 0.94$, based on the lack of variability on 10 yr baseline and the lack of optical polarization (Berriman et al. 1990; McDowell et al. 1995). Another example of similar spectral peculiarity is the high accretion rate quasar PHL 1811 at $z = 0.19$ (Leighly et al. 2007a). Samples of radio-quiet BLO candidates at lower redshifts ($z < 2.2$) were found in the Sloan Digital Sky Survey (SDSS; York et al. 2000), by Collinge et al. (2005) and Anderson et al. (2007), and were termed 'weak-line-quasars' (WLQs). As a result, dozens of WLQs marked by abnormally weak broad emission lines (i.e. rest-frame EW < 15.4 Å for the Lyα+NV emission-line complex; Diamond-Stanic et al. 2009) have been reported (e.g. Fan et al. 1999, 2006; Anderson et al. 2001; Hall et al. 2002, 2004; Collinge et al. 2005; Reimers et al. 2005; Schneider et al. 2005, 2007; Shemmer et al. 2006, 2009; Ganguly et al. 2007; Leighly et al. 2007b; Diamond-Stanic et al. 2009; Hryniewicz et al. 2010; Plotkin et al. 2010a,b; Wu et al. 2011).

Although the above studies have revealed many WLQs that are indeed radio-quiet (e.g. Plotkin et al. 2010b), they are commonly identified not as BLOs but RQQs having abnormally weak emission lines. This is because, in contrast to BLOs (and much like RQQs), the radio-quiet WLQs (RQWLQs) are found to exhibit low optical polarization (Smith et al. 2007) and mild optical continuum variability on time-scales ranging from days to years (Plotkin et al. 2010b). This is further supported by the similarity observed between the UV–optical spectral indices, α, of WLQs and RQQs. For RQQs the median value of α is −0.52 (Diamond-Stanic et al. 2009; Plotkin et al. 2010a), as against −1.15 for BLO candidates (e.g. Plotkin et al. 2010a). The reason for the abnormally weak line emission in WLQs is yet to be fully understood, but the explanations proposed basically fall into two categories. One possible cause of the abnormality is the high mass of the central black hole (BH; $M_{\rm BH} > 3 \times 10^9\,{\rm M}_{\odot}$) which can result in an accretion disc too cold to emit strongly the ionizing UV photons, even when its optical output is high (Laor & Davis 2011; see also Plotkin et al. 2010a).

★ E-mail: hum@aries.res.in

Alternatively, the covering factor of the broad-line region (BLR) in WLQs could be at least an order of magnitude smaller compared to the normal QSOs (e.g. Nikołajuk & Walter 2012). An extreme version of this scenario is that in WLQs the accretion disc is relatively recently established and hence a significant BLR is yet to develop (Hryniewicz et al. 2010; Liu & Zhang 2011). Conceivably, a poor BLR could also result from the weakness of the radiation-pressure-driven wind when the AGN is operating at an exceptionally low accretion rate ($<10^{-2}$ to $10^{-3}\dot{M}_{\rm Edd}$; Nicastro, Martocchia & Matt 2003; see also Elitzur & Ho 2009).

While the above-mentioned limited empirical evidences and theoretical scenarios are consistent with the quasar interpretation of the bulk of the WLQ population, they do not rule out the possibility of a small subset of the population being, in fact, the long-sought radio-quiet BLOs in which optical emission arises predominantly from a relativistic jet of synchrotron radiation (e.g. Stocke & Perrenod 1981; Diamond-Stanic et al. 2009; Plotkin et al. 2010a and references therein; see also Stalin & Srianand 2005).

One strategy to pursue such a search is to characterize the intranight optical variability (INOV) of RQWLQs. It is well established that normal BLOs (which are always radio-loud) exhibit a distinctly stronger INOV, both in amplitude (ψ) and duty cycle (DC), as compared to quasars, specially their radio-quiet majority, RQQs (e.g. Gopal-Krishna et al. 2003; Stalin et al. 2004a; Gupta & Joshi 2005; Carini et al. 2007; Goyal et al. 2012). From this it is evident that INOV properties can be a strong discriminator between blazars and other powerful AGN, both radio-loud and radio-quiet (e.g. Stalin et al. 2004a; Goyal et al. 2012). The impetus behind our new programme, therefore, is to characterize the INOV behaviour of RQWLQs and the first results are presented here.

2 THE SAMPLE OF RADIO-QUIET WLQs

Our sample for INOV monitoring (Table 1) was derived from the list of 86 radio-quiet WLQs published in table 6 of Plotkin et al. (2010a), based on the SDSS Data Release 7 (DR7; Abazajian et al. 2009). Out of that list, we included in our sample all 18 objects brighter than $R \sim 18.5$ which are classified as 'high-confidence BL Lac candidate'. Thus far, we have been able to carry out intranight monitoring of only eight of these sources in 13 sessions and the results are reported here.

Table 1. The eight RQWLQs studied in the present work.

IAU name (1)	RA (J2000) (h m s) (2)	Dec. (J2000) (° ′ ″) (3)	B (mag) (4)	z (5)
J081250.79+522531.05	08 12 50.80	+52 25 31	18.30	1.152
J084424.20+124546.00	08 44 24.20	+12 45 46	18.28	2.466
J090107.60+384659.00	09 01 07.60	+38 46 59	18.21	1.329
J121929.50+471522.00	12 19 29.50	+47 15 22	17.66	1.336
J125219.50+264053.00	12 52 19.50	+26 40 53	17.94	1.292
J142943.60+385932.00	14 29 43.60	+38 59 32	17.56	0.925
J153044.10+231014.00	15 30 44.10	+23 10 14	17.32	1.040
J161245.68+511817.31	16 12 45.68	+51 18 17	17.70	1.595

2.1 Photometric observations

Continuous monitoring of each RQWLQ was done, mainly using the 1.3-m optical telescope (hereafter 1.3-m DFOT)[1] of the Aryabhatta Research Institute of Observational Sciences (ARIES), located at Devasthal, India (Sagar et al. 2011). DFOT is a fast beam ($f/4$) optical telescope with a pointing accuracy better than 10 arcsec rms. The telescope is equipped with Andor CCD having 2048 × 2048 pixels of 13.5 µm size, resulting in field of view of 18 arcmin on the sky. The CCD is read out with 31 and 1000 kHz speeds, with the corresponding system rms noise of 2.5, 7e$^-$ and gain of 0.7, 2e$^-$/analog-to-digital unit (ADU). The camera is cooled down thermoelectrically to −85°C. We performed continuous monitoring of each source for about 4 h in the SDSS–r passband at which our CCD system has maximum sensitivity. For achieving signal-to-noise ratio (S/N) greater than 25–30 our typical exposure time was set between 5 and 8 min. The typical seeing full width at half-maximum (FWHM) during our monitoring sessions was 2 arcsec, adequate for these point-like sources.

One of the RQWLQ (J125219.47+264053.9) was also monitored with the 1.04-m Sampurnanand telescope (ST) located at ARIES, Nainital, India. Another RQWLQ (J090107.60+384659.0) was also monitored using the 2-m IUCAA Girawali Observatory (IGO) telescope located near Pune, India. The ST has Ritchey–Chrétien (RC) optics with a $f/13$ beam (Sagar 1999). The detector was a cryogenically cooled 2048 × 2048 chip mounted at the Cassegrain focus. This chip has a readout noise of 5.3e$^-$ pixel^{-1} and a gain of 10 e$^-$ ADU^{-1} in the slow readout mode. Each pixel has an area of 24 µm^2 which corresponds to 0.37 arcsec^2 on the sky, covering a total field of 13 × 13 arcmin^2. Our observations were carried out in 2 × 2 binned mode to improve the S/N, and Cousins R filters were used.

The 2-m IGO telescope has an RC design with a $f/10$ beam at the Cassegrain focus.[2] The detector was a cryogenically cooled 2110 × 2048 chip mounted at the Cassegrain focus. The pixel area is 15 µm^2, so that the image scale of 0.27 arcsec pixel^{-1} covers an area of 10 × 10 arcmin^2 on the sky. The readout noise of this CCD is 4.0e$^-$ pixel^{-1} and the gain is 1.5e$^-$ ADU^{-1}. The CCD was used in an unbinned mode with Cousins R filters.

In our sample selection, care was taken to ensure the availability of at least two, but usually more, comparison stars on the CCD frame that were within about 1 mag of the target RQWLQ. This allowed us to identify and discount any comparison star which itself varied during a given night and hence ensured reliable differential photometry of the RQWLQ.

2.2 Data reduction

All pre-processing of the images (bias subtraction, flat-fielding and cosmic ray removal) was carried out using the standard tasks available in the data reduction software IRAF.[3] Instrumental magnitudes of the comparison stars and the target source were measured from the frames using the Dominion Astronomical Observatory Photometry (DAOPHOT II) software designed for concentric circular aperture photometric technique (Stetson 1992, 1987). As a check on the possible effects of any seeing variations, the aperture photometry was carried out with four aperture radii, 1 × FWHM, 2 × FWHM, 3 × FWHM and 4 × FWHM, where the seeing disc radius (= FWHM/2)

[1] Devsthal Fast Optical Telescope.
[2] http://www.iucaa.ernet.in/~itp/igoweb/igo_tele_and_inst.htm
[3] Image Reduction and Analysis Facility (http://iraf.noao.edu/).

for each CCD frame was determined using five fairly bright stars on the frame. The data reduced using the four aperture radii were found to be in generally good agreement. However, the best S/N for the differential light curves (DLCs) was nearly always found for aperture radii of $\sim 2 \times$ FWHM, so we adopted that aperture for our final analysis.

To derive the DLCs of a given target RQWLQ, we selected two steady comparison stars present within the CCD frames, on the basis of their proximity to the target source, both in location and magnitude. Coordinates of the comparison star pair selected for each RQWLQ are given in Table 2. The $g - r$ colour difference for our 'quasar–star' and 'star–star' pairs is always <1.5, with a median value of 0.54 (column 7, Table 2). Detailed analyses by Carini et al. (1992) and Stalin et al. (2004a) show that colour difference of this magnitude should produce negligible effect on the DLCs as the atmospheric attenuation changes during a monitoring session.

Since the selected comparison stars are non-varying, as judged from the steadiness of their DLCs, any sharp fluctuation over a single temporal bin was taken to arise due to improper removal of cosmic rays, or some unknown instrumental effect, and such outlier data points (deviating by more than 3σ from the mean) were removed from the affected DLCs, by applying a mean clip algorithm. In practice, such outliers were quite rare and never exceeded two data points for any DLC, as displayed in Fig. 1. Finally, in order to enhance the SNR, without incurring significant loss of time resolution, we have taken three point box average of each DLC.

3 ANALYSIS

Conventionally, the presence of INOV in a DLC is quantified using C-statistics (Jang & Miller 1997). However, recently de Diego (2010) has pointed out that this is not a valid test as it is based on ratio of two standard deviations which (unlike variance) are not linear operators and the nominal critical value used for confirming the presence of variability (i.e. 2.576) is usually too conservative. He has therefore advocated more powerful statistical tests, namely, the one-way analysis of variance (ANOVA) and the F test. However, a proper use of the ANOVA test requires a rather large number of

Table 2. Basic parameters and observing dates of the eight RQWLQs and their comparison stars.

IAU name (1)	Date (dd.mm.yyyy) (2)	RA (J2000) ($^{h\ m\ s}$) (3)	Dec. (J2000) ($^{\circ\ \prime\ \prime\prime}$) (4)	g (mag) (5)	r (mag) (6)	$g - r$ (mag) (7)
J081250.79+522531.0	23.01.2012	08 12 50.79	+52 25 31.0	18.30	18.05	0.25
S1		08 12 50.27	+52 26 32.8	17.48	17.05	0.44
S2		08 12 29.42	+52 20 49.9	19.51	18.09	1.43
J084424.24+124546.5	26.02.2012	08 44 24.24	+12 45 46.5	18.29	17.91	0.37
S1		08 44 30.80	+12 41 24.8	19.42	18.00	1.42
S2		08 44 39.26	+12 44 54.6	18.27	17.87	0.40
J090107.64+384658.8	27.02.2012	09 01 07.64	+38 46 58.8	18.25	18.15	0.09
S1		09 01 21.12	+38 42 14.1	18.93	17.69	1.24
S2		09 00 43.86	+38 51 42.0	17.92	17.47	0.44
J090107.64+384658.8	16.03.2012	09 01 07.64	+38 46 58.8	18.25	18.15	0.09
S1		09 01 00.15	+38 47 09.7	19.64	18.27	1.37
S2		09 00 59.94	+38 47 51.4	18.77	18.00	0.77
J121929.45+471522.8	26.02.2012	12 19 29.45	+47 15 22.8	17.65	17.53	0.12
S1		12 19 33.79	+47 17 04.5	17.28	16.72	0.56
S2		12 20 11.17	+47 13 09.2	17.88	16.83	1.05
J121929.45+471522.8	27.04.2012	12 19 29.45	+47 15 22.8	17.65	17.53	0.12
S1		12 19 57.89	+47 14 56.9	18.66	17.35	1.31
S2		12 19 02.24	+47 12 18.2	18.42	17.18	1.24
J125219.47+264053.9	25.02.2012	12 52 19.47	+26 40 53.9	17.94	17.70	0.24
S1		12 52 37.93	+26 37 47.6	17.52	16.98	0.54
S2		12 52 14.26	+26 39 11.5	18.43	17.15	1.28
J125219.47+264053.9	23.03.2012	12 52 19.47	+26 40 53.9	17.94	17.70	0.24
S1		12 52 37.93	+26 37 47.6	17.52	16.98	0.54
S2		12 52 14.26	+26 39 11.5	18.43	17.15	1.28
J125219.47+264053.9	19.05.2012	12 52 19.47	+26 40 53.9	17.94	17.70	0.24
S1		12 52 23.82	+26 41 42.6	16.71	16.42	0.29
S2		12 52 00.81	+26 43 17.5	16.93	15.86	1.07
J142943.64+385932.2	27.02.2012	14 29 43.64	+38 59 32.2	17.56	17.55	0.01
S1		14 30 00.65	+38 57 21.4	19.08	17.62	1.46
S2		14 29 30.69	+39 01 14.2	18.16	17.00	1.16
J153044.08+231013.4	27.04.2012	15 30 44.08	+23 10 13.4	17.83	17.59	0.24
S1		15 30 09.51	+23 11 52.9	18.46	17.15	1.31
S2		15 30 47.76	+23 06 10.4	17.79	17.19	0.60
J153044.08+231013.4	19.05.2012	15 30 44.08	+23 10 13.4	17.83	17.59	0.24
S1		15 30 09.46	+23 11 07.1	17.29	16.71	0.58
S2		15 30 57.70	+23 07 42.3	17.01	16.65	0.36
J161245.68+511816.9	18.05.2012	16 12 45.68	+51 18 16.9	17.89	17.72	0.17
S1		16 12 26.15	+51 22 14.6	18.08	16.69	1.39
S2		16 12 48.21	+51 18 37.1	15.33	14.94	0.39

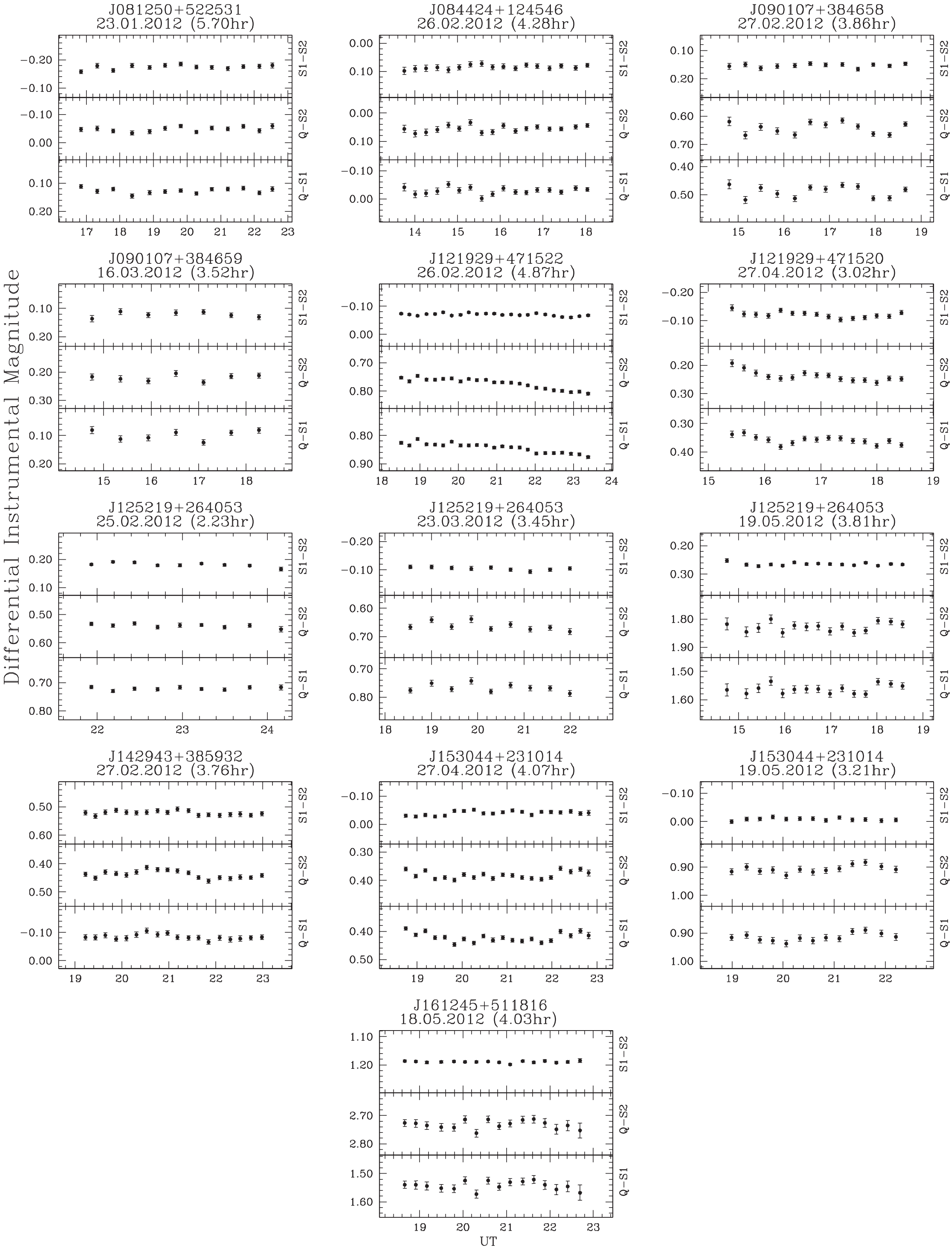

Figure 1. DLCs, after three point box average, for the eight RQWLQs in our sample. The name of the quasar along with the date and duration of the monitoring session are given at the top of each panel. In each panel the upper DLC is derived using the two comparison stars, while the lower two DLCs are the 'quasar–star' DLCs, as defined in the labels on the right-hand side. Any likely outlier point (at $>3\sigma$) in the DLCs are marked with crosses (see Section 2) and those points are excluded from the statistical analysis.

data points in the DLC, so as to have several points within each subgroup used for the analysis; this is not feasible for our light curves which typically have only around 15–20 data points each. Therefore, in this study we shall rely on the F test which is based on the ratio of variances as, $F = \mathrm{variance}_{\mathrm{(observed)}}/\mathrm{variance}_{\mathrm{(expected)}}$ (de Diego 2010). Two versions of this test employed in the recent literature are (i) the standard F test (hereinafter F^{η} test; Goyal et al. 2012) and (ii) scaled F test (hereinafter F^{κ} test; Joshi et al. 2011). In this work we have subjected all our DLCs to both these statistical tests, as discussed below.

An important point to be borne in mind while applying the F^{η} test is that the photometric errors, as returned by the routines in the IRAF and DAOPHOT softwares, are normally underestimated by a factor η ranging between 1.3 and 1.75, as found in independent studies (e.g. Gopal-Krishna, Sagar & Wiita 1995; Garcia et al. 1999; Sagar et al. 2004; Stalin et al. 2004b; Bachev, Strigachev & Semkov 2005). In a recent analysis of 73 DLCs derived for 73 pairs of ‘steady’ stars monitored on as many nights, Goyal et al. (2012) estimated the best-fitting value of η to be 1.5. (see also Section 4). The F^{η} statistics can be expressed as

$$F_1^{\eta} = \frac{\sigma^2_{(\mathrm{q-s1})}}{\eta^2 \left\langle \sigma^2_{\mathrm{q-s1}} \right\rangle}, \quad F_2^{\eta} = \frac{\sigma^2_{(\mathrm{q-s2})}}{\eta^2 \left\langle \sigma^2_{\mathrm{q-s2}} \right\rangle}, \quad F_{\mathrm{s1-s2}}^{\eta} = \frac{\sigma^2_{(\mathrm{s1-s2})}}{\eta^2 \left\langle \sigma^2_{\mathrm{s1-s2}} \right\rangle}, \tag{1}$$

where $\sigma^2_{(\mathrm{q-s1})}$, $\sigma^2_{(\mathrm{q-s2})}$ and $\sigma^2_{(\mathrm{s1-s2})}$ are the variances of the ‘quasar–star1’, ‘quasar–star2’ and ‘star1–star2’ DLCs and $\langle \sigma^2_{\mathrm{q-s1}} \rangle = \sum_{i=0}^{N} \sigma^2_{i,\mathrm{err}}(\mathrm{q-s1})/N$, $\langle \sigma^2_{\mathrm{q-s2}} \rangle$ and $\langle \sigma^2_{\mathrm{s1-s2}} \rangle$ are the mean square (formal) rms errors of the individual data points in the ‘quasar–star1’, ‘quasar–star2’ and ‘star1–star2’ DLCs, respectively. η is the scaling factor (=1.5; cf. Goyal et al. 2012), introduced to account for the underestimation of photometric rms errors returned by the photometry algorithms used here, as mentioned above.

The F values computed using equation (1) were then compared individually with the critical F value, $F^{(\alpha)}_{\nu_{\mathrm{qs}},\nu_{\mathrm{ss}}}$, where α is the significance level set for the test, and ν_{qs} and ν_{ss} are the degrees of freedom of the ‘quasar–star’ and ‘star–star’ DLCs, respectively. The smaller the α, the more improbable is the result to arise from chance. For the present study, we have used two significance levels, $\alpha = 0.01$ and 0.05, which correspond to confidence levels of greater than 99 and 95 per cent, respectively. If F is found to exceed the critical value, the null hypothesis (i.e. no variability) is discarded to the corresponding level of confidence. We have computed separately the F values for the ‘quasar–star1’ and ‘quasar–star2’ DLCs (i.e. F_1^{η} and F_2^{η}) from equation (1). Thus, for a given monitoring session, a RQWLQ is marked as *variable* (‘V’) if for both its DLCs F value $\geq F_{\mathrm{c}}(0.99)$, which corresponds to a confidence level $\geq$99 per cent; *non-variable* (‘NV’) if even one of the two DLCs is found to have F value less than $F_{\mathrm{c}}(0.95)$. The remaining cases are termed as *probably variable* (‘PV’).

An alternative approach to quantify the INOV status of a DLC has been followed in Joshi et al. (2011), the ‘scaled F test’. Instead of η, this test relies on a factor κ equal to the ratio of the mean square rms errors of the data points in the quasar DLC relative to a comparison star and in the DLC of that star relative to the other comparison star. This parameter is intended to correct for any bias which may arise due to some systematic difference between the photometric errors of the data points in the ‘quasar–star’ and ‘star–star’ DLCs (e.g. due to a brightness mismatch between the quasar and the comparison star(s)). Thus, in this ‘scaled’ F test,

$$F_1^{\kappa} = \frac{\mathrm{var(q-s1)}}{\kappa\ \mathrm{var(s1-s2)}}, \qquad F_2^{\kappa} = \frac{\mathrm{var(q-s2)}}{\kappa\ \mathrm{var(s1-s2)}}, \tag{2}$$

with κ, defined as

$$\kappa = \left[\frac{\sum_{i=0}^{N} \sigma^2_{i,\mathrm{err}}(\mathrm{q-s})/N}{\sum_{i=0}^{N} \sigma^2_{i,\mathrm{err}}(\mathrm{s1-s2})/N} \right] \equiv \frac{\langle \sigma^2_{\mathrm{q-s}} \rangle}{\langle \sigma^2_{\mathrm{s1-s2}} \rangle}, \tag{3}$$

where $\sigma_{i,\mathrm{err}}(\mathrm{q-s})$ and $\sigma_{i,\mathrm{err}}(\mathrm{s1-s2})$ are, respectively, the rms errors on individual points of the ‘quasar–star’ and ‘star–star’ DLCs, as returned by the DAOPHOT/IRAF routine.

The threshold criteria for inferring the INOV status of a DLC from its computed F value in this F^{κ} test is identical to that adopted above for the F^{η} test. The inferred INOV status of the DLCs of each RQWLQ, relative to two comparison stars, is presented in Table 3.

Table 3. Observational details and INOV results for the sample of eight RQWLQs.

RQWLQ	Date	Tel.	T	N^a	F-test values		INOV status^b		INOV amplitude	$\sqrt{\kappa}^c$	$\sqrt{\langle \sigma^2_{i,\mathrm{err}} \rangle}$
	(dd.mm.yyyy)	used	(h)		F_1^{η}, F_2^{η}	F_1^{κ}, F_2^{κ}	F_{η} test	F_{κ} test	ψ_1, ψ_2 (per cent)		(q–s)
(1)	(2)	(3)	(4)	(5)	(6)	(7)	(8)	(9)	(10)	(11)	(12)
J081250.79+522530.9	23.01.2012	DFOT	5.70	13	0.77, 0.59	1.59, 1.21	NV, NV	NV, NV	3.03, 1.94	0.99	0.01
J084424.24+124546.5	26.02.2012	DFOT	4.28	17	0.65, 0.63	2.83, 2.74	NV, NV	PV, PV	4.49, 3.49	1.00	0.01
J090107.64+384658.8	27.02.2012	DFOT	3.86	12	1.62, 1.67	5.81, 6.00	NV, NV	V, V	5.00, 4.74	1.41	0.01
J090107.64+384658.8	16.03.2012	IGO	3.52	07	1.11, 0.57	2.66, 1.36	NV, NV	NV, NV	3.73, 2.37	1.07	0.01
J121929.45+471522.8	26.02.2012	DFOT	4.87	23	4.85, 6.23	5.55, 7.13	V, V	V, V	6.35, 6.14	1.52	0.01
J121929.45+471522.8	27.04.2012	DFOT	3.02	15	1.01, 1.65	1.34, 2.18	NV, NV	NV, NV	4.56, 6.64	1.13	0.01
J125219.47+264053.9	25.02.2012	DFOT	2.23	09	0.24, 0.37	0.21, 0.32	NV, NV	NV, NV	0.36, 1.39	1.43	0.01
J125219.47+264053.9	23.03.2012	ST	3.45	09	0.98, 1.02	3.00, 3.12	NV, NV	NV, NV	3.93, 3.87	1.51	0.01
J125219.47+264053.9	19.05.2012	DFOT	3.81	15	0.52, 0.54	0.92, 0.95	NV, NV	NV, NV	3.43, 3.76	3.17	0.01
J142943.64+385932.2	27.02.2012	DFOT	3.76	18	0.46, 1.41	1.23, 3.76	NV, NV	NV, V	3.49, 4.58	1.05	0.01
J153044.07+231013.5	27.04.2012	DFOT	4.07	20	2.13, 1.48	3.07, 2.13	NV, NV	V, NV	5.46, 3.81	1.21	0.01
J153044.07+231013.5	19.05.2012	DFOT	3.21	13	0.67, 0.58	3.63, 3.12	NV, NV	PV, PV	4.19, 4.02	1.62	0.01
J161245.68+511817.3	18.05.2012	DFOT	4.03	16	0.44, 0.44	1.81, 1.83	NV, NV	NV, NV	4.02, 3.87	3.57	0.02

^{a}The number of data points after three point box average.
^{b}V = variable, i.e. confidence level $\geq$0.99; PV = probable variable, i.e. 0.95–0.99 confidence level; NV = non-variable, i.e. confidence level <0.95. Variability status values based on quasar–star1 and quasar–star2 pairs are separated by a comma.
^{c}Here $\kappa = \langle \sigma^2_{\mathrm{q-s}} \rangle / \langle \sigma^2_{\mathrm{s1-s2}} \rangle$ (as in equation 3) is used to scale the variance of star1–star2 DLCs for the scaled F test.

In the first five columns, we list the name of the RQWLQ, date of its monitoring, telescope used, duration of monitoring and the number, N, of data points in the DLCs relative to the two comparison stars (s1 and s2). The next two columns give the computed F values, based on the F^{η} test and F^{κ} tests. Columns 8 and 9 mention the INOV status of the two DLCs of the RQWLQ, as inferred from the F^{η} test and F^{κ} test, respectively. Column 10 gives the INOV amplitudes ψ derived from the two DLCs of the RQWLQ, based on the definition given by Romero, Cellone & Combi (1999):

$$\psi = \sqrt{(D_{\max} - D_{\min})^2 - 2\sigma^2}, \quad (4)$$

with $D_{\min,\,\max}$ = minimum (maximum) in the RQWLQ DLC and $\sigma^2 = \eta^2 \langle \sigma^2_{\text{q-s}} \rangle$, where, η =1.5 (Goyal et al. 2012). Column 11 lists the square root of the scaling factor, κ (equation 3), which has been used to scale the variance of the star–star DLCs while computing the F value in the scaled F test (equation 2). The last column gives our averaged photometric error $\sigma_{i,\text{err}}$(q–s) in the 'quasar−star' DLCs (i.e. mean value for q–s1 and q–s2 DLCs), which typically lies between 0.01 and 0.02 mag.

3.1 The INOV duty cycle

To recapitulate, a RQWLQ in a given session is marked as *variable* ('V') if its DLCs relative to the two comparison stars are both found to have F value $\geq F_c(0.99)$, which corresponds to a confidence level ≥99 per cent; *non-variable* ('NV') if even one of the two DLCs is found to have F value less than $F_c(0.95)$. The remaining cases are marked as *probably variable* ('PV').

The DC of INOV was computed using the definition by Romero et al. (1999):

$$\text{DC} = 100 \frac{\sum_{i=1}^{n} N_i (1/\Delta t_i)}{\sum_{i=1}^{n} (1/\Delta t_i)} \text{ per cent}, \quad (5)$$

where $\Delta t_i = \Delta t_{i,\,\text{obs}} (1+z)^{-1}$ is duration of the monitoring session of a source on the ith night, corrected for its cosmological redshift, z. Since the duration of the observing session for a given source differs from night to night, the computation of DC has been weighted by the actual monitoring duration Δt_i on the ith night. N_i was set equal to 1, if INOV was detected (i.e. 'V'), otherwise N_i was taken as zero.

4 DISCUSSION AND CONCLUSIONS

The present study marks the beginning of a systematic investigation of the INOV properties of RQWLQs. This initial attempt is based on a modest-size sample containing eight RQWLQs for which the derived results are presented in Table 3. Using the F^{κ} test we obtained an INOV DC of ∼13 per cent which rises to ∼30 per cent if the two cases of probable INOV ('PV') are included. On the other hand, the F^{η} test yields for the same data set an INOV DC of ∼6 per cent (taking the best-fitting value of $\eta = 1.5$, Section 3). Thus, taken together, the two F tests lead to an average INOV DC of around 9 per cent for RQWLQs, for monitoring sessions lasting $\gtrsim$3.5 h. In order to assess the effect of possible uncertainty in the η factor (Section 3), we have repeated the F^{η} test for the entire sample, taking two extreme values of η (=1.3 and 1.75), as reported in the literature (e.g. Gopal-Krishna et al. 1995; Garcia et al. 1999; Stalin et al. 2004a; Bachev et al. 2005). The computed INOV DCs for both these extreme values of η are still 6 per cent, i.e. the same as that estimated above taking $\eta = 1.5$, the best-fitting estimate given in Goyal et al. (2012). Thus, the F^{η} test is found to give consistent results over the maximum plausible range of uncertainty in η.

At this point it seems worthwhile to also mention the DC estimate based on the more conservative, but hitherto much more extensively used C test (Section 3). We find that the only change to Table 3, resulting from the application of C test to our data set is that INOV status of the WLQ J121929.45+471522.8 on 2012 February 26 changes from 'V' to 'PV'. This leaves no clear incidence of INOV detection in the present data. Treating 'PV' cases as 'V' yields an INOV DC of ∼6 per cent, which would clearly be an upper limit, albeit using a small sample. Our subsequent discussion will only be based on the results obtained from the F test as it is believed to be a more powerful test (Diego 2010; Section 3).

Bearing in mind the modest size of our RQWLQ sample at this stage, we now attempt a comparison of the INOV DC with the estimates available for RQQs and other AGN classes, such as non-blazar-type flat-spectrum radio quasars (FSRQs) and blazars. INOV DCs for these AGN classes have been extensively reported in the literature (e.g. Stalin et al. 2004b; Goyal et al. 2012), mostly based on DLCs longer than ∼4 h (which broadly holds even for the present DLCs of RQWLQs, as well). One limitation encountered in making the comparison is that for the observations of all these other AGN types, an INOV detection threshold (ψ_{lim}) of 1–2 per cent had typically been achieved (at least in our programme from ARIES, Section 1). Being 1–2 mag fainter, the INOV detection threshold reached for the present sample of RQWLQs is less deep ($\psi_{\text{lim}} \sim$ 4–5 per cent, Table 3). Thus, for the purpose of comparison with the afore-mentioned other AGN types, our present estimate of INOV DC for RQWLQs (∼9 per cent) must be treated as a lower limit. It would be very interesting to check if a factor of 2–3 improvement in ψ_{lim} would lead to a much higher INOV DC for RQWLQs, perhaps even approaching the level of ∼50 per cent which is established for strong INOV (i.e. $\psi > 3$ per cent) of blazars (BL Lacs and high-polarization radio quasars) when they are monitored for $\gtrsim$4 h (e.g. Gopal-Krishna et al. 2003, 2011; Sagar et al. 2004; Stalin et al. 2004a,b; Goyal et al. 2012). The DC for strong INOV is found to be only ∼7 per cent for non-blazar type FSRQs (based on the F^{η} test; e.g. Goyal et al. 2012) and practically zero for RQQs since they are not known to show INOV with $\psi > 3$ per cent (e.g. Gopal-Krishna et al. 2003; Stalin et al. 2004a, 2005; Goyal et al. 2007). Thus, one indication emerging from this first INOV observations of radio-quiet WLQs is that their INOV level, as a class, is likely to be significantly stronger in comparison to the general population of RQQs, and indeed similar that that known for non-blazar-type radio quasars (FSRQs). It remains to be seen whether on attaining a matching INOV detection threshold $\psi_{\text{lim}} \sim$ 1–2 per cent, the INOV activity level of RQWLQs will be found to be stronger, perhaps approaching the high levels exhibited by blazars (e.g. Goyal et al. 2012 and references therein). This remains an outstanding question to be pursued, in view of its potential for unravelling the nature of WLQs and for the key question whether radio-quiet BL Lacs at all exist (Section 1). It may be noted here that a hint that, compared to normal RQQs, RQWLQs may show stronger optical/UV variability on *year-like* time-scale, has been reported by Stalin & Srianand (2005); though it is based on monitoring of just one RQWLQ (SDSS J153259.96−003944.1 at $z = 4.67$).

To summarize, the twin objectives pursued in this exploratory, first INOV study of RQWLQs are (a) to find cases of strong INOV ($\psi > 3$ per cent), any such RQWLQs would be outstanding candidates for the putative radio-quiet BL Lacs, and (b) to quantify the INOV DC for the class of RQWLQs, for both strong and weaker

INOV. In our program we have so far been able to cover only a modest-size sample containing eight RQWLQs, each monitored in at least one session lasting $\gtrsim$3.5 h. This has led to the result that the DC of strong INOV in this class of AGN seems to be higher than that known for RQQs and is similar to that known for (non-blazar) FSRQs. This early indication provides impetus to continue this programme, in particular, to check if blazar-like INOV levels occur in some RQWLQs. To attain the required observational capability, a factor of $\gtrsim$2 improvement in the INOV detection threshold would be needed and we are attempting to achieve this by monitoring relatively bright RQWLQs on dark nights, possibly using a telescope larger than the newly installed 1.3-m DFOT used in the present work.

ACKNOWLEDGMENTS

We would like to thank Dr Arti Goyal for helpful discussions and the scientific staff and observers at the 1.3-m DFOT telescope, ARIES (Nainital, India) for the assistance with the observations.

REFERENCES

Abazajian K. N. et al., 2009, ApJS, 182, 543
Anderson S. F. et al., 2001, AJ, 122, 503
Anderson S. F. et al., 2007, AJ, 133, 313
Bachev R., Strigachev A., Semkov E., 2005, MNRAS, 358, 774
Berriman G., Schmidt G. D., West S. C., Stockman H. S., 1990, ApJS, 74, 869
Carini M. T., Miller H. R., Noble J. C., Goodrich B. D., 1992, AJ, 104, 15
Carini M. T., Noble J. C., Taylor R., Culler R., 2007, AJ, 133, 303
Collinge M. J. et al., 2005, AJ, 129, 2542
de Diego J. A., 2010, AJ, 139, 1269
Diamond-Stanic A. M. et al., 2009, ApJ, 699, 782
Elitzur M., Ho L. C., 2009, ApJ, 701, L91
Fan X. et al., 1999, ApJ, 526, L57
Fan X. et al., 2006, AJ, 131, 1203
Ganguly R. et al., 2007, AJ, 133, 479
Garcia A., Sodré L., Jablonski F. J., Terlevich R. J., 1999, MNRAS, 309, 803
Gopal-Krishna, Sagar R., Wiita P. J., 1995, MNRAS, 274, 701
Gopal-Krishna, Stalin C. S., Sagar R., Wiita P. J., 2003, ApJ, 586, L25
Gopal-Krishna, Goyal A., Joshi S., Karthick C., Sagar R., Wiita P. J., Anupama G. C., Sahu D. K., 2011, MNRAS, 416, 101
Goyal A., Gopal-Krishna, Sagar R., Anupama G. C., Sahu D. K., 2007, Bull. Astron. Soc. India, 35, 141
Goyal A., Gopal-Krishna, Wiita P. J., Anupama G. C., Sahu D. K., Sagar R., Joshi S., 2012, A&A, 544, A37
Gupta A. C., Joshi U. C., 2005, A&A, 440, 855
Hall P. B. et al., 2002, ApJS, 141, 267
Hall P. B. et al., 2004, AJ, 127, 3146
Hryniewicz K., Czerny B., Nikołajuk M., Kuraszkiewicz J., 2010, MNRAS, 404, 2028
Jang M., Miller H. R., 1997, AJ, 114, 565
Jannuzi B. T., Green R. F., French H., 1993, ApJ, 404, 100
Jiang L., Fan X., Ivezić Ž., Richards G. T., Schneider D. P., Strauss M. A., Kelly B. C., 2007, ApJ, 656, 680
Joshi R., Chand H., Gupta A. C., Wiita P. J., 2011, MNRAS, 412, 2717
Kellermann K. I., Sramek R., Schmidt M., Shaffer D. B., Green R., 1989, AJ, 98, 1195
Laor A., Davis S. W., 2011, MNRAS, 417, 681
Leighly K. M., Halpern J. P., Jenkins E. B., Casebeer D., 2007a, ApJS, 173, 1
Leighly K. M., Halpern J. P., Jenkins E. B., Grupe D., Choi J., Prescott K. B., 2007b, ApJ, 663, 103
Liu Y., Zhang S. N., 2011, ApJ, 728, L44
Londish D., Heidt J., Boyle B. J., Croom S. M., Kedziora-Chudczer L., 2004, MNRAS, 352, 903
McDowell J. C., Canizares C., Elvis M., Lawrence A., Markoff S., Mathur S., Wilkes B. J., 1995, ApJ, 450, 585
Nicastro F., Martocchia A., Matt G., 2003, ApJ, 589, L13
Nikołajuk M., Walter R., 2012, MNRAS, 420, 2518
Plotkin R. M. et al., 2010a, AJ, 139, 390
Plotkin R. M., Anderson S. F., Brandt W. N., Diamond-Stanic A. M., Fan X., MacLeod C. L., Schneider D. P., Shemmer O., 2010b, ApJ, 721, 562
Reimers D., Janknecht E., Fechner C., Agafonova I. I., Levshakov S. A., Lopez S., 2005, A&A, 435, 17
Romero G. E., Cellone S. A., Combi J. A., 1999, A&AS, 135, 477
Sagar R., Stalin C. S., Gopal-Krishna, Wiita P. J., 2004, MNRAS, 348, 176
Sagar R., 1999, Curr. Sci., 77, 643
Sagar R. et al., 2011, Curr. Sci., 101, 8
Schneider D. P. et al., 2005, AJ, 130, 367
Schneider D. P. et al., 2007, AJ, 134, 102
Shemmer O. et al., 2006, ApJ, 644, 86
Shemmer O., Brandt W. N., Anderson S. F., Diamond-Stanic A. M., Fan X., Richards G. T., Schneider D. P., Strauss M. A., 2009, ApJ, 696, 580
Shen Y. et al., 2011, ApJS, 194, 45
Smith P. S., Williams G. G., Schmidt G. D., Diamond-Stanic A. M., Means D. L., 2007, ApJ, 663, 118
Stalin C. S., Srianand R., 2005, MNRAS, 359, 1022
Stalin C. S., Gopal-Krishna, Sagar R., Wiita P. J., 2004a, MNRAS, 350, 175
Stalin C. S., Gopal-Krishna, Sagar R., Wiita P. J., 2004b, JA&A, 25, 1
Stalin C. S., Gupta A. C., Gopal-Krishna, Wiita P. J., Sagar R., 2005, MNRAS, 356, 607
Stetson P. B., 1987, PASP, 99, 191
Stetson P. B., 1992, in Worrall D. M., Biemesderfer C., Barnes J., eds, ASP Conf. Ser. Vol. 25, Astronomical Data Analysis Software and Systems I. Astron. Soc. Pac., San Francisco, p. 297
Stocke J. T., Perrenod S. C., 1981, ApJ, 245, 375
Stocke J. T., Morris S. L., Gioia I., Maccacaro T., Schild R. E., Wolter A., 1990, ApJ, 348, 141
Stocke J. T., Morris S. L., Weymann R. J., Foltz C. B., 1992, ApJ, 396, 487
Wu J. et al., 2011, ApJ, 736, 28
York D. G. et al., 2000, AJ, 120, 1579

This paper has been typeset from a TEX/LATEX file prepared by the author.